2
Open-Channel Hydraulics: From Then to Now and Beyond

Xiaofeng Liu

CONTENTS

Abstract As a subdiscipline of water resources engineering, open-channel hydraulics is of critical importance to human history. This chapter starts with a brief history of open-channel hydraulics. Then the fundamental concepts in open-channel hydraulics (specific energy, momentum, and resistance) are introduced. The new development on the subject of open-channel flow modeling is discussed at some length. A general introduction on 1D, 2D, and 3D computer modeling and examples will be given. Despite the tremendous progress made in the past, modern and future challenges include revisiting past projects which were designed using less than ideal standards, effect of climate variability, and natural open channels in the arid environment. The chapter concludes with a discussion of potential future directions.

Key Words Open-channel hydraulics • Numerical modeling • Turbulence • Sediment transport.

1. INTRODUCTION

Open-channel hydraulics is a critical subdiscipline in the area of water resources engineering that has been practiced successfully throughout the settled parts of the world long before recorded history. Functional systems of open channels, of course, also predate modern theory and those modern essentials for design and analysis such as the computer.

From: *Handbook of Environmental Engineering, Volume 15: Modern Water Resources Engineering*
Edited by: L.K. Wang and C.T. Yang, DOI 10.1007/978-1-62703-595-8_2,

An appropriate beginning of this very brief review of the importance of open channels in prehistory and history is to quote Hunter Rouse [1] who wrote in 1957, "A major task in dealing with modern times is. . .to separate the vast amount of chaff from the essential grain." The advent of the information age has only added validity to this statement. However, it is worth briefly reflecting on the essential role water resources engineering, in general, and open channels, in specific, have played in human development. In c. 4000 BC, the Egyptians dammed the Nile in the vicinity of Memphis (a short distance south of Cairo) in part to divert flood waters to prehistoric Lake Moeris which could store vast quantities of water for irrigation. In c. 2300 BC the canal connecting the Nile and Lake Moeris was deepened and widened to form what is now known as *Bahr Yussef*. The purposes of this open-channel-reservoir system were to control the flooding of the Nile, regulate the water level of the Nile during dry seasons, and irrigate the surrounding area [1]. In c. 1800 BC, Egyptians also built a canal connecting the Nile River and Red Sea. The existence of this canal was quoted by Aristotle, Strabo, and Pliny the Elder. It should be observed that apparently the Red Sea then tended further north then than it does today. The history of what today is known as the Middle East is replete with systems of dams and open-channel systems that sustained agriculture and allowed the development and growth of urban areas. Similar major systems also were undertaken in China, India, and Pakistan.

Certainly the best known contribution of the Romans, from the viewpoint of open-channel hydraulics, was the aqueduct. Throughout the Roman world, water was collected at springs and/or wells and transmitted by open channels to urban areas where it was distributed to consumers often by pressurized pipes. The Roman consumer was charged for the use of the resource so the system could be sustained. Although it cannot be known with certainty, Roman water resources engineers and their equally skilled predecessors likely had very little theoretical knowledge. However, they knew a slight slope was required for water to flow and that water will not rise above its initial elevation without the addition of energy.

After the fall of the Roman Empire, the "Dark Ages" descended in the west during which there was minimal recorded scientific and engineering progress. The Dark Ages were followed by the Renaissance and the rise of observational science. It was during this period that individuals of the stature of Leonardo da Vinci (1452–1519) made direct and critical contributions to hydraulic engineering. Regarding Leonardo's discussion of continuity in the riverine environment Hunter Rouse said,

> . . .he did it with such originality and clarity that the principle might justifiably bear his name. ([1], p. 49)

Following the major contributions of Newton to mechanics in the seventeenth century, Daniel Bernoulli, Leonhard Euler, and Jean le Rond d'Alembert made notable theoretical contributions in the field of hydrodynamics, which are well known. During the same period, Antoine Chezy and Robert Manning, as discussed in a subsequent section, made critical and lasting contributions to open-channel hydraulics.

In what was to become the United States, the planning of major water resources projects involving open channels began in Colonial times. In the eighteenth century, waterways were the most efficient means of transport and, hence, essential to commerce. In 1763, George Washington suggested draining the Great Dismal Swamp and connecting Chesapeake Bay in

Virginia with Albemarle Sound in North Carolina by a canal obviating the need to transport goods along the dangerous Carolina coast. In 1784, the Dismal Swamp Canal Company was formed and work on the canal began in 1793. The canal was dug completely by hand since this was before the age of steam power, and most of labor force was slaves. The 22 mile (35 km) long canal finally opened in 1805, and the canal, operated by the US Army Corps of Engineers, is still used.

Construction of the Erie Canal began on July 4, 1817, and the men who planned and oversaw its construction (James Geddes, Benjamin Wright, Canvass White, and Nathan Roberts to name just a few) were talented novices rather than trained civil engineers. Yet these individuals planned, designed, and constructed a project that contained hydraulic engineering structures that remain notable today such as the structure carrying the canal over the Niagara Escarpment at Lockport, New York. The canal, 363 miles (584 km) long, was completed in October 1826 without the benefit of power equipment. Many of the laborers on this project were newly arrived Scots-Irish immigrants. The canal was enlarged between 1834 and 1865 and was replaced by the New York State Barge Canal in 1918. It is pertinent to observe that the Erie Canal resulted in the building of competing transportation systems including the Baltimore and Ohio Railroad, the Mohawk and Hudson Railroad to name just two.

The Dismal Swamp and Erie Canals are only the best known of the many canals built in the United States in the late eighteenth and early nineteenth centuries as they were the interstate highways of the time. Agricultural and urban development west of the Rocky Mountains in semiarid and arid environments required canals convey water from the mountains where water is abundant to where it was needed for crops and people. Certainly one of the best known American water resources projects of the twentieth century is Los Angeles Aqueduct that conveys water by gravity from the Owens Valley in the Sierra Nevada Mountains to Los Angeles. This project led to what are known as the California water wars. Conceptually, the project began in 1898 when Frederick Eaton appointed William Mulholland as head of the Los Angeles Department of Water and Power. The Los Angeles envisioned by Eaton and Mulholland bore no relationship to the small coastal community it was at the turn of the twentieth century. In the early 1900s, the Owens Valley was a rich agricultural region with the needed irrigation water being provided by a number of small irrigation districts rather than a large district as had been recommended by John Wesley Powell. Eaton, Mulholland, and other Los Angeles visionaries (or scoundrels depending on your viewpoint) recognized the opportunity that was available for the taking. By 1905, Los Angeles using bribery, intimidation, subterfuge, and political influence up as high as President Theodore Roosevelt owned sufficient land and water rights in the Valley to justify the construction of the aqueduct.

From 1905 through 1913 Mulholland directed the construction of the 233 mile (375 km) aqueduct. By 1920s so much water was being exported from the Owens Valley that "the Switzerland of California" was becoming a desert, and the Valley residents took up armed rebellion. The rebellion was for naught because by 1928 Los Angeles owned most of the water in the Valley and only minimal agriculture was left. The reader is encouraged to consult refs.

[2, 3] for more details of this critical and controversial water resources project which was part of the plot in the Academy Award winning movie *Chinatown*.

In 1970, Los Angeles completed a second aqueduct to export even more water from the Valley. In response to various lawsuits, Los Angeles has put forth various plans to "rewater" the lower Owens River and bar all future development on its holding in the Owens Valley. Thus, the controversy over a simple gravity-driven system of open channels and pipes has spanned a full century and will continue into the future.

By the beginning of the twentieth century, most of the critical analytic tools required to design and build effective and fully operational open-channel systems for transportation and water supply were available. One of the best known and respected engineers involved in early twentieth-century open-channel hydraulics was Boris A. Bakhmeteff. Bakhmeteff was a civil engineering educator and consultant in St. Petersburg, Russia, before he became the Kerensky government's ambassador to the United States. After the fall of the Kerensky government, he remained in the United States. Bakhmeteff in 1912 published in Russian a book on open channels and subsequently published a much enlarged version in English.

Many mark the beginning of modern open-channel hydraulics with the publication of Bakhmeteff's *Hydraulics of Open Channel Flow*. In the following sections of this chapter, the fundamentals (specific energy, momentum, and resistance) are briefly discussed, and then the subject of modeling of open-channel flow is discussed at some length. The chapter concludes with a discussion of potential future directions.

1.1. Specific Energy

If the longitudinal slope of the channel is small, energy in an open channel is given by

$$H = z + y + \frac{u^2}{2g} \tag{2.1}$$

where H = total energy, z = elevation of the channel bottom above a datum, y = depth of flow, and u = cross-sectional average velocity. It is pertinent to note the modifications required if the slope is not small and development and use of the energy correction factor as the flow departs from being adequately described as one-dimensional. If the channel bottom slope is less than 1:10 (5.75°), the pressure in the flow is hydrostatic and corrections to the computed depths of flow are not required [4]. Channels with longitudinal slopes greater than 1:10 are rare, but the engineer needs to be aware that when modeling such channels the estimated depth may require adjustment [4].

As flow cross sections depart from simple geometric shapes such as rectangular and trapezoidal to include overbank flow areas, average velocity becomes less valid as a descriptor of the kinetic energy of the flow. The kinetic energy correction factor (also known as the velocity weighting coefficient) is intended to allow the one-dimensional energy equation to be used in situations that depart from being one-dimensional. Setting the actual kinetic energy of a flow equal to the kinetic energy of the one-dimensional idealization

$$\alpha\gamma\frac{\overline{u^3}}{2g}A = \iint_A \gamma\frac{u^3}{2g}\mathrm{d}A \tag{2.2}$$

$$\alpha = \frac{\iint_A \gamma u^3 \mathrm{d}A}{\gamma\overline{u^3}A} \tag{2.3}$$

where $\boldsymbol{\alpha}$ = kinetic energy correction factor, $\overline{u}$ = cross-sectional average velocity, A = area, and u = velocity. In an analogous fashion, a momentum correction factor, $\boldsymbol{\beta}$, can be derived or

$$\beta = \frac{\iint_A \rho u^2 \mathrm{d}A}{\rho\overline{u^2}A} \tag{2.4}$$

With regard to $\boldsymbol{\alpha}$ and $\boldsymbol{\beta}$, the following observations are pertinent. First, for uniform flow, $\boldsymbol{\alpha} = \boldsymbol{\beta} = 1$. Second, for a given channel section and velocity distribution, $\boldsymbol{\alpha}$ is more sensitive to variations in velocity than $\boldsymbol{\beta}$. Third, as noted previously, $\boldsymbol{\alpha}$ and $\boldsymbol{\beta}$ are of importance when the channel consists of a primary channel and sub-channels and/or berms and floodplains. In such cases judgment must be used to decide if two-dimensional modeling should be used.

By definition, specific energy is

$$E = y + \frac{u^2}{2g}. \tag{2.5}$$

And for a rectangular channel of width b and a flow per unit width q, the specific energy equation becomes

$$E = \ y + \frac{q^2}{2gy^2} \tag{2.6}$$

$$E - y = \frac{q^2}{2gy^2} \tag{2.7}$$

$$(E - y)y^2 = \frac{q^2}{2g} \tag{2.8}$$

For a specified flow rate and channel width, the right-hand side of the equation is constant and the curve has asymptotes

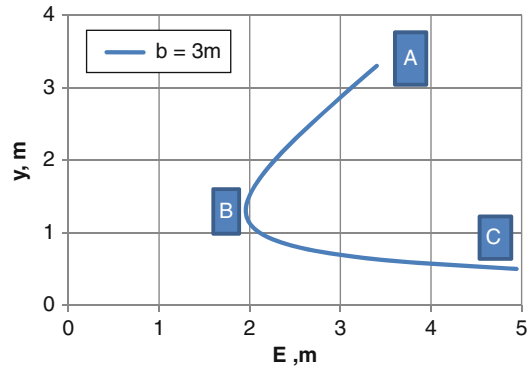

Fig. 2.1. Specific energy as a function of depth for a rectangular channel with $Q = 14$ m^3/s and $b = 3$ m.

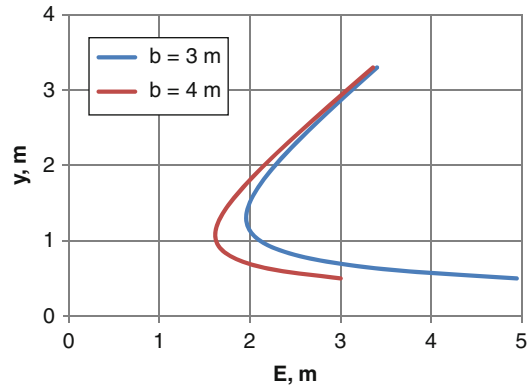

Fig. 2.2. Specific energy as a function of depth for a rectangular channel with $Q = 14$ m^3/s, $b = 3$ m, and $b = 4$ m.

$$y = 0 \tag{2.9}$$

$$(E - y) = 0. \tag{2.10}$$

It is also noted the equation has valid solutions in the first and third quadrants with only those in the first quadrant being of practical interest. Figure 2.1 is a plot of y vs. E for a flow of 14 m^3/s in a rectangular with a bottom width of 3 m. With regard to this figure, the following observations are pertinent. First, Pt. B is the only point where for a given value of E, there is a single depth of flow. At Pt. B the depth of flow is critical and the Froude number has a value of 1. Second, depths and velocities of flow associated with branch "BA" are subcritical, Froude number less than 1. Third, depths and velocities of flow associated with branch "BC" are supercritical, Froude number greater than 1. Fourth, for a given flow rate, there is a different $E - y$ for each channel width, see Fig. 2.2. Fifth, from a design viewpoint, flows that are either strongly sub- or supercritical are desirable because near the critical point a change in flow regime can lead to a large change in depth.

Specific energy provides the basis for estimating the variation of channel shape and longitudinal slope on the depth of flow. Taking the derivative of (2.1) with respect to

longitudinal distance × yields

$$\frac{dH}{dx} = \frac{dy}{dx} + \frac{dz}{dx} + \frac{d\left(\frac{u^2}{2g}\right)}{dx} \tag{2.11}$$

and recognizing

$$\frac{dH}{dx} = -S_f$$

and

$$\frac{dz}{dx} = -S_o.$$

For a given flow rate Q,

$$\frac{d\left(\frac{u^2}{2g}\right)}{dx} = -\frac{Q^2}{gA^3}\frac{dA}{dy}\frac{dy}{dx} = -\frac{Q^2T}{gA^3}\frac{dy}{dx} = -F^2\frac{dy}{dx}.$$

Then substituting in (2.11) and simplifying yields

$$\frac{dy}{dx} = \frac{S_o - s_f}{1 - F^2} \tag{2.12}$$

Equation (2.12) describes the variation of the depth of flow with distance in steady open-channel flow.

1.2. Specific Momentum (Specific Force)

In considering the application of Newton's second law of motion to steady open-channel flow, it is convenient to define specific momentum (specific force) or

$$M_i = \overline{z_i}A_i + \frac{Q^2}{gA_i}$$

where i = section identification, $\overline{z_i}$ = distance to the centroid of flow area A, and Q = flow rate. Then for a control volume where Station 1 is upstream and Station 2 downstream, Newton's second law can be written as

$$\frac{F}{\gamma} = M_1 - M_2$$

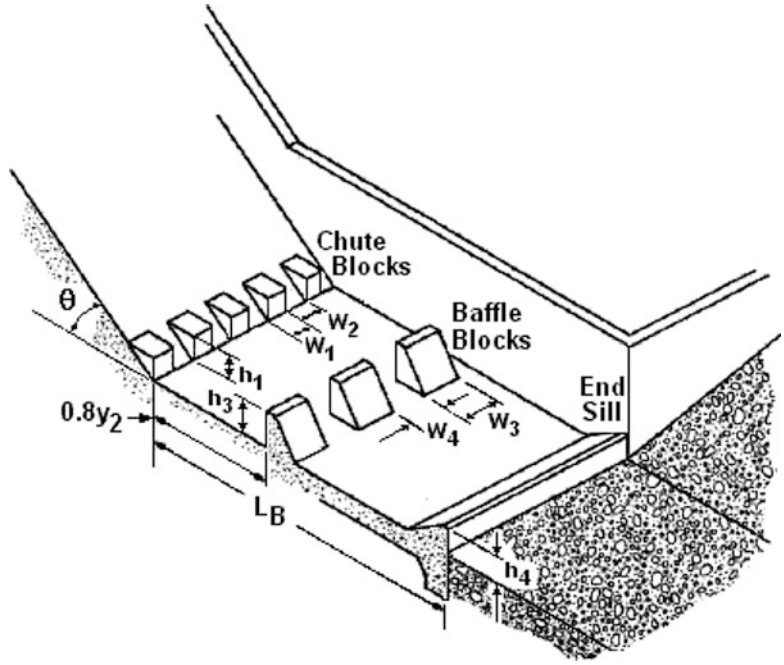

Fig. 2.3. United States Bureau of Reclamation (USBR) Type III stilling basin [5].

where F = unknown force or forces acting in the control volume. At this point, three possibilities must be considered

$\Delta E = 0$
e.g., a sluice gate
$F \neq 0$

$\Delta E \neq 0$
e.g., simple hydraulic jump , Fig. 2.3
$F = 0$

$\Delta E \neq 0$
e.g., hydraulic jump assisted by stilling basin , Fig. 2.4
$F \neq 0$

For simplicity, the following discussion will be limited to results for rectangular channels. The widest used results of specific momentum analysis are the results for hydraulic jumps. The applications of hydraulic jumps in open-channel hydraulics are many and include:

Dissipation of energy in flows over dams, weirs, and other hydraulic structures;
Maintenance of high water levels in channels for water distribution;
Increase the discharge of a sluice gate by repelling the downstream tailwater;
Reduction of the uplift pressure under a structure by raising the water depth on the apron;
Hydraulic mixing of chemicals for water purification or treatment; and
Aeration and dechlorination of flows.

Fig. 2.4. Simple hydraulic jump occurring in a flood mitigation channel in Albuquerque, New Mexico, USA (Photo courtesy of Albuquerque Metropolitan Arroyo Flood Control Authority).

If the jump occurs in a horizontal, rectangular channel without the assistance structural appurtenances such as chute blocks or sills, then

$$M_1 = M_2$$

and the classic equation for sequent depth results or

$$\frac{y_2}{y_1} = 0.5\left(\sqrt{1 + \ 8F_1^2} - 1\right)$$

where y_1 and y_2 = depths of flow at upstream Station 1 and downstream Station 2, respectively, and F_1 = Froude number at Station 1. The sequent depth equation is often interpreted in a much too simple fashion; that is, if the supercritical conditions of flow at Station 1 are as described by y_1 and F_1, then the depth of flow after the hydraulic jump will be y_2 tacitly assuming a hydraulic jump occurs. In point of fact, a hydraulic jump will not occur unless the engineer causes depth y_2 to exist. Controlling the location of a hydraulic jump is a critical engineering and often requires the use of hydraulic structures such as the US Bureau of Reclamation Type III stilling basin shown in Fig. 2.3. Guidance regarding the design of stilling basins is available in agency design manuals (e.g., [5]) and standard engineering handbooks (e.g., [6]).

1.3. Resistance

From the viewpoint of water resources engineering and open-channel hydraulics, the latter eighteenth and early nineteenth centuries were an age of achievement yielding fundamental

equations produced by men whose names are familiar to every hydraulic engineer—in particular, Chezy and Manning.

Antoine Chezy was born in 1718 at Chalon-sur-Marne, France, and died in 1797. In 1760, the City of Paris was experiencing a water supply problem apparently related to the poor operation of its pumps. Seeking a solution, the City approached the *Academie des Sciences* which recommended, among other alternatives, water be brought to the City by a gravity canal from the nearby Yvette River. In 1768, the City moved forward, and Chezy was tasked to design the cross section of the canal and determine its discharge. As would be today, this was a critical engineering task since if the section was too small, the water required would not be delivered, and if it was too large, the right of way required would be too large. Public works projects then had critics, just as they do today. Chezy's review of the literature apparently found nothing that adequately addressed the issue; and therefore, he initiated his own investigation. It is relevant to note that there had been discussions regarding the relationship between the velocity and slope and the effect of the bed on velocity [1]. The report containing his recommendations was lost, but the files of the agency, Ponts et Chaussees, contain the original manuscript [1] and it is there that the Chezy Equation is put forward. The final report on the Yvette Project only contained the results of Chezy's computations and made no mention of the method used.

It is appropriate to mention that the French Revolution halted the Yvette River project. Chezy's simple, elegant approach to calculating uniform flow went unrecognized by his peers, and Chezy himself would have died in poverty except for the intercession of one of his students, Baron Riche de Prony which led to Chezy's appointment as the director of the Ecole Ponts et Chaussees. According to refs. [1, 7], the Chezy Equation was not widely used until it was published at the end of the nineteenth century by the well-known American hydraulic engineer Clemens Herschel [8]. However, Herschel seems to contradict this stating ". . .called the Chezy formula and well known in the engineering literature of Germany, France, England, and the United States."

Robert Manning was born in Normandy, France, the year following Waterloo, 1816, and died in 1897. In 1889, Manning, a professor at the Royal College of Dublin (Ireland) and chief engineer of the Office of Public Works responsible for various drainage, inland navigation, and harbor projects, presented a paper entitled "On the Flow of Water in Open Channels and Pipes" to the Institution of Civil Engineers in Ireland; and in this paper, the Manning equation was presented which Manning believed corrected defects in previous resistance models. It is pertinent to note that Manning was a self-taught hydraulic engineer with no formal training in engineering. Manning was apparently not aware that a French engineer, Philippe Gaspard Gauckler, had put forward essentially the same model in c. 1868 [7]. The popularity and widespread use of the Manning resistance formulation has been ascribed to its publication in a popular late nineteenth-century textbook by Flamant [7, 9].

The Manning Equation has always had its detractors, but none was any more critical than Robert Manning himself. According to [1], Manning had the following in his original paper:

> . . .if modern formulae are empirical with scarcely an exception, and are not homogeneous, or even dimensional, then it is obvious that the truth of any such equation must altogether depend on that of the observations themselves, and it cannot in strictness be applied to a single case outside them.

Thus, Manning was quite aware of the limitations of his formulation which was in better agreement with data available than any other approach. Manning's second objection to his formulation was the need to extract a cubic root which was not easily done before the electronic age. In fact, Fischenich [10] pointed to the publication of King's *Handbook* [11] in 1918 with tabulation of the two-thirds power of numbers between 0.01 and 10 to firmly establishing the Manning resistance model preferred approach in American engineering practice.

It is pertinent to observe that Manning then abandoned the approach that bears his name and developed a dimensionally homogeneous equation which was apparently never widely used [1].

1.4. Rise of the Computer

The effort and time required to correctly plan, analyze, and design complex systems of open channels prior to the advent and widespread availability of digital computers was staggering. Given the scale, scope, and success of the projects discussed in the introduction, the resourcefulness and ingenuity of those involved in those projects must be recognized. Certainly, the most notable and significant advances in open-channel hydraulics since the 1960s have been due to the widespread availability of relatively inexpensive and increasing powerful computers and software. The models discussed in the next section, and the insights they provide for effective analysis and design of open channels would not be possible without the modern computer. However, these computational advances have also been accompanied by concerns, and two of the most notable are the following. First, other than knowing the effect of gravity on water, many modern hydraulic engineers have no inherent understanding of flow in open channels. That is, for these engineers, critical physical processes have been reduced to abstract algorithms, and they have no basis for judging the reasonableness of the digital output. Second, many modern engineers are unable to effectively function without sophisticated calculators and computers. Thus, as is the case with any significant technical leap forward, there are unanticipated problems that must be addressed.

2. NUMERICAL MODELING OF OPEN-CHANNEL HYDRAULICS

2.1. Review of Numerical Modeling of Open-Channel Flows

With the widespread availability of powerful personal computers and the development of high-performance computers (HPC), numerical models for hydraulic engineering have gained popularity during the last several decades. This popularity is also propelled by the development of new numerical methods and efficient numerical schemes where hydraulic phenomena and processes with more complexity can be modeled. Along with theoretical and experimental research, computational models have grown to an important branch of hydraulics.

Numerical modeling of open channels has progressed from the original one-dimensional open-channel flow equations to three-dimensional free surface flows. The following is a brief overview of the achievements in the computer modeling of open-channel flow.

To perform numerical modeling for open-channel flows, as well as in other areas of fluid mechanics, the basic process includes preprocessing, computation, and post-processing. At the preprocessing stage, the majority of the work is to prepare the data in the format required by the specific numerical code. In the case of three-dimensional modeling, the preprocessing stage can be a major portion of the whole process. One of the difficulties during this stage is to generate a reasonable mesh that represents the domain of interest and has a good quality. Most of the commercial codes have their own preprocessing and mesh generation tools. There are also some independent meshing tools available which specialize in making high-quality meshes and are easy to use. Since there are many numerical models and each employs different numerical schemes, they require different mesh formats and vary on the tolerance on mesh quality; it is impossible to list each of them. Readers should refer to the documentations of these codes. One general suggestion is to make a mesh with good quality and at affordable resolution.

Depending on the dimensionality of the numerical models for open-channel flows, they can be classified into different categories, i.e., one-, two-, and three-dimensional models. Examples include the HEC series of pseudo-1D models, FESWMS-2DH from Federal Highway Administration (FHWA), and open-source HydroSed2D based on 2D depth-averaged shallow-water equations. The examples of fully three-dimensional computational fluid dynamics (CFD) models include commercial codes such as Fluent, Flow3D, Phoenics, CD-adapco, and the popular OpenFOAM from the open-source community.

Despite the variety and availability of different computer codes, there still exist challenges, as well as opportunities, for the numerical modeling of open-channel flows: (1) uncertainties in input data such as bathymetry, resistance law and roughness, vegetation, and flow measurement data; (2) computational domain and temporal span are large, which dictates that computational demand is high, especially for 3D modeling; (3) multiple scales needs to be resolved (in open-channel flow, it is often required or at least desirable to capture the global mean flow and the local variations); and (4) model calibration needs extensive data which are not always available.

In the following, numerical models (1D, 2D, and 3D) and their example applications are introduced. Depending on the physical scales, each category of models has its applications. For large-scale (such as river reach) modeling, 1D and 2D modes may be the right choice since they are faster and require less data input and yet reveal the overall hydraulic behavior. For localized, small-scale flow phenomenon, such as open-channel flow around hydraulic structures, flow over bedforms, and sediment elements, a fully 3D model is necessary and affordable.

2.2. *One-Dimensional Modeling of Open-Channel Flows*

2.2.1. Governing Equations for One-Dimensional Open-Channel Flow

The general equations for unsteady nonuniform open-channel flows are the Saint-Venant equations or the dynamic wave equations. The derivation of the Saint-Venant equations is based on the shallow-water approximation where the vertical pressure distribution is hydrostatic and the vertical acceleration is small. It is also assumed that the channel bottom slope is

small such that $S = \sin\theta$, where θ is the angle of the channel bed relative to the horizontal. It is also important to note that the resistance law used for the unsteady flow is assumed to be the same for steady flow; and therefore, the Manning and Chezy equations can be used.

The continuity equation which describes the water mass balance has the form

$$\frac{\partial A}{\partial t} + \frac{\partial Q}{\partial x} - q_1 = 0 \tag{2.13}$$

and the momentum equation which describes the force balance of a control volume has the form

$$\frac{\partial Q}{\partial t} + \frac{\partial}{\partial x}(QV) = gA(S_0 - S_f) \tag{2.14}$$

where A is the cross-sectional area of the flow which depends of the geometry of the channel cross section and the flow depth, V is the average velocity perpendicular to the cross section, and $Q = AV$ is the flow rate. q_1 in the continuity equations is the lateral inflow rate per unit channel length. In the momentum equations, $S_0 = -\partial z/\partial x$ is the water surface slope and z is the free surface elevation. S_f is the friction slope which is a function of flow and stage. The friction slope is determined by the resistance equation, such as Manning and Chezy equations. In derivation of (2.14), it is assumed the momentum associated with the lateral inflow can be neglected.

2.2.2. Numerical Solutions

Due to its simplicity and one dimensionality, the finite-difference method can be used to approximate the derivatives (both spatial and temporal) in the Saint-Venant equations. The spatial discretization for derivatives and source terms can be evaluated at the beginning of a time step (explicit) or the end of a time step (implicit). Different temporal discretization schemes can be used on different terms in the governing equations giving the mixed explicit-implicit formulations. The second mostly used scheme for the derivatives is the so-called method of characteristics (MOC) where the derivatives are calculated along the characteristic grid lines. The governing equations, which are partial differential equations (PDEs), need to be transformed along the characteristic curves [11]. The transformed equations are ordinary differential equations (ODE) which are readily solved. Once the ODEs are solved, the solution to the original PDEs for the 1D unsteady flow equations can be obtained. MOC is used in special cases where the transient is important, for example, dam-break flows. Since the governing equations are PDEs in general, other discretization schemes (such as finite element, finite volume, and spectral methods) could also be used. However, they are not used as often as the finite-difference method and MOC.

Instead of solving the full continuity and momentum equations, simplified versions can be solved without losing the dominant mechanisms. In the simplified versions, some of the terms have been omitted from the full equations or one of the equations is not used. When only the continuity equation is used (with the momentum equation ignored), it is called hydrologic

routing. When both equations are solved, it is called hydraulic routing [12]. In hydraulic routing, there are three sub-routing schemes, i.e., kinematic, diffusion, and dynamic routings. The kinematic routing considers only the balance between gravity and flow resistance, and diffusion routing ignores the inertia terms (temporal and convective accelerations). The dynamic routing includes all terms. When applying these different routing schemes, it is important to keep in mind the assumption that the neglected terms are relatively small comparing to others. If this assumption is not satisfied, the results will not capture the physical process.

To fully describe the details of finite difference and the MOC that needs a lengthy derivation, interested readers could consult references which are devoted to this topic.

There are many commercial and public domain codes available for the simulation of 1D open-channel flows which implement the various numerical schemes mentioned before. One of the most widely used models is HEC-RAS [4], which uses the finite-difference method. It has three basic hydraulic analysis components which comprise steady flow computations, unsteady flow computations, and movable boundary sediment transport computations. The software integrates the graphical user interface (GUI) with the three components as well as the data management system to facilitate the ease of use.

2.2.3. Examples

Due to its simplicity and efficiency, 1D open-channel flow models have been used widely for engineering design and flood risk analysis. The most popular 1D model, HEC-RAS, has been used by the industry and government agencies for open-channel design. The typical outputs of the model would be river stage, flow, and resistance (Figs. 2.5 and 2.6).

In flood prediction and mapping, it is very convenient to combine the hydraulic model results with geographic information system (GIS). For example, in [14], HEC-RAS model was integrated in GIS to predict the areal coverage of the flood over real terrains. It used high-resolution elevation data in the stream and the relatively low-resolution data in the floodplain. The resulting model was used for the Waller Creek in Austin, Texas.

2.3. Two-Dimensional Modeling of Open-Channel Flows

Two-dimensional modeling of open-channel flows usually uses the depth-averaged shallow-water equations (SWEs) where the vertical acceleration of the fluid is ignored. The governing equations for the one-dimensional modeling in the previous section can be viewed as a special case of SWEs where one spatial derivative vanishes. Both 1D and 2D modeling equations belong to the broad category of hyperbolic partial differential equations which has a natural connection with conservation laws.

It is noted that there are also two-dimensional models with one dimension being the vertical and the other one being along the river. This modeling methodology is applicable when the variation across the river is small and the emphasis is to model the vertical motion and transport. Although equaly important, this vertical 2D modeling will not be introduced and this section will only treat two-dimensional depth-averaged modeling using shallow-water equations.

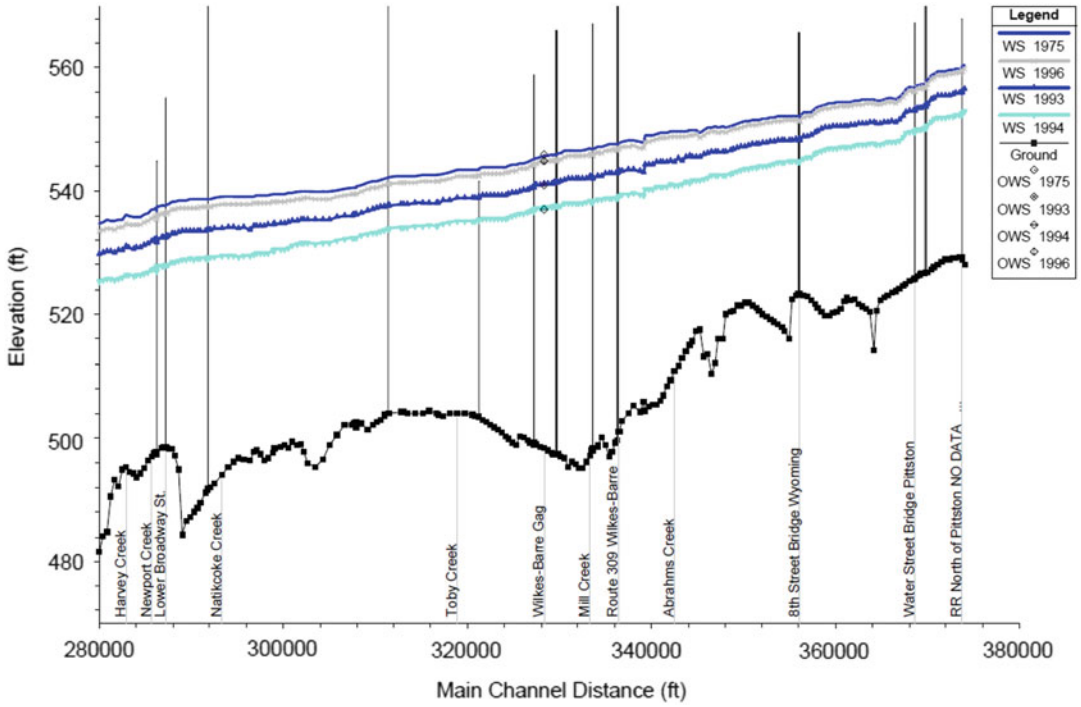

Fig. 2.5. Example outputs of water surface profiles for different flood events [13].

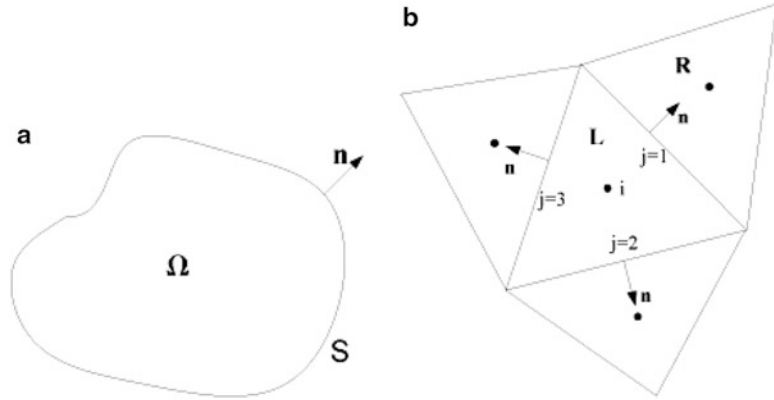

Fig. 2.6. Numerical schemes for 2D SWEs: (**a**) Control volume for the finite volume method. (**b**) Unstructured mesh topology.

As for general partial differential equations, numerical schemes (such as finite difference, finite volume, finite element methods) have been used to discretize the governing equations (e.g., [15–19]). Finite volume and finite element methods are more popular in solving SWEs since they use unstructured mesh which is ideal for complex domains. On the other hand, regular two-dimensional Cartesian grid can be used to model rectangular domains or the

governing equations can be transformed into curvilinear orthogonal coordinate systems for irregular domains (e.g., [20]). Other noval techniques for the meshing and representation of the computational domain have been proposed and successfully used. For example, an adaptive quadtree meshing and modeling method was proposed in [21] where any two-dimensional boundary topology can be approximated with the capability of enriching and coarsening dynamically.

Available codes for two-dimensional depth-averaged modeling include TELEMAC [22], TUFLOW [23], and HydroSed2D [18]. For the purpose of illustration, in the following, the shallow-water equations will be introduced and the finite volume method used for discretization will be elaborated. The scheme is exactly the one used in HydroSed2D and is similar to the ones used by others.

2.3.1. Governing Equations of Depth-Averaged Shallow-Water Equations

Two-dimensional shallow-water equations can be written in normal conservation law form as

$$\frac{\partial h}{\partial t}+\frac{\partial (uh)}{\partial x}+\frac{\partial (vh)}{\partial y}=0 \tag{2.15}$$

$$\frac{\partial (uh)}{\partial t}+\frac{\partial \left(u^2h+\frac{1}{2}gh^2\right)}{\partial x}+\frac{\partial (uvh)}{\partial y}=ghS_{ox}-ghS_{fx}+\frac{\tau_{wx}}{\rho}+hfu \tag{2.16}$$

$$\frac{\partial (vh)}{\partial t}+\frac{\partial (uvh)}{\partial x}+\frac{\partial \left(v^2h+\frac{1}{2}gh^2\right)}{\partial y}=ghS_{oy}-ghS_{fy}+\frac{\tau_{wy}}{\rho}-hfv \tag{2.17}$$

where h is the water depth, u and v are the depth-averaged velocities in x and y directions respectively, g is the gravity constant, ρ is the water density, τ_{wx} and τ_{wy} are surface wind shear stresses, f is the Coriolis parameter, and ν is the kinematic eddy viscosity. S_{ox} and S_{oy} are the bed slopes in the x and y directions; S_{fx} and S_{fy} are the friction slopes in the x and y directions, respectively, which can be estimated using Manning's formula

$$S_{fx}=n^2u\sqrt{u^2+v^2} \tag{2.18}$$

$$S_{fy}=n^2v\sqrt{u^2+v^2} \tag{2.19}$$

where n is Manning's roughness coefficient.

The 2D SWEs can be written in compact integral form as

$$\frac{\partial}{\partial t}\int_{\Omega}q\mathrm{d}\Omega+\int_{\Omega}\left(\frac{\partial f}{\partial x}+\frac{\partial g}{\partial y}\right)\mathrm{d}\Omega=\int_{\Omega}R\mathrm{d}\Omega \tag{2.20}$$

where

$$\boldsymbol{q} = \begin{pmatrix} h \\ uh \\ vh \end{pmatrix}, \quad \boldsymbol{f} = \begin{pmatrix} uh \\ u^2h + \frac{1}{2}gh^2 - \nu h\frac{\partial u}{\partial x} \\ uvh - \nu h\frac{\partial v}{\partial x} \end{pmatrix}, \quad \boldsymbol{g} = \begin{pmatrix} vh \\ uvh - \nu h\frac{\partial v}{\partial x} \\ u^2h + \frac{1}{2}gh^2 - \nu h\frac{\partial u}{\partial x} \end{pmatrix}$$

$$\boldsymbol{R} = \begin{bmatrix} 0 & ghS_{ox} - ghS_{fx} + \frac{\tau_{wx}}{\rho} + hfv & ghS_{oy} - ghS_{fy} + \frac{\tau_{wy}}{\rho} - hfu \end{bmatrix}^T$$

2.3.2. Numerical Schemes

The Godunov scheme is used to solve the conservative variables as defined in the previous section [24]. The basic idea of Godunov scheme is to assume the piecewise constant distribution of these conservative variables over each mesh cell and the time evolution is achieved by solving the Riemann problem at the cell–cell interfaces [25]. To improve the accuracy, the piecewise constant distribution can be replaced by high-order interpolations leading to higher spatial accuracy. Higher order schemes are important to capture transcritical flows and discontinuities such as dam-break/levee-breach flows.

Using Green's theorem, the divergence term of (2.20) can be transformed into line integral and the vector form of the governing equations becomes

$$\frac{\partial}{\partial t}\int_{\Omega} \boldsymbol{q}\mathrm{d}\Omega + \oint_S \hat{\boldsymbol{f}}\mathrm{d}S = \int_{\Omega} \boldsymbol{R}\mathrm{d}\Omega \tag{2.21}$$

where S is the boundary of the control volume Ω and $\hat{\boldsymbol{f}}$ is the flux vector given by

$$\hat{f} = [f \quad g] \cdot n = fn_x + gn_y \tag{2.22}$$

Here, $\boldsymbol{n}$ is the unit outward normal vector which has the Cartesian components n_x and n_y. The flux vector $\hat{\boldsymbol{f}}$ can be further split into inviscid and viscous fluxes as

$$\hat{f} = f^I - \nu f^V \tag{2.23}$$

$$f^I = \begin{pmatrix} uhn_x + vhn_y \\ \left(u^2h + \frac{1}{2}gh^2\right)n_x + uvhn_y \\ uvhn_x + \left(v^2h + \frac{1}{2}gh^2\right)n_y \end{pmatrix}, \quad f^V = \begin{pmatrix} 0 \\ h\frac{\partial u}{\partial x}n_x + h\frac{\partial u}{\partial y}n_y \\ h\frac{\partial v}{\partial x}n_x + h\frac{\partial v}{\partial y}n_y \end{pmatrix} \tag{2.24}$$

Using standard finite volume method, (2.21) can be written as

$$\left.\frac{\partial Vq}{\partial t}\right|_i = \oint_S \hat{f}\,\mathrm{d}S + V_i R_i, \text{where } \oint_S \hat{f}\,\mathrm{d}S = \sum_j \hat{f}_{i,j}\,\Delta l_j \tag{2.25}$$

where V is the area of the control volume and variables with subscript i represent the values stored at the center of the cell. $\hat{f}_{i,j}$ is the interfacial flux between current cell i, and the neighbor j, Δl_j is the length of the side sharing with cell j.

The representation of the different values across a boundary between two adjacent cells leads to the Riemann problem. There are many solvers (exact and approximate) to solve the Riemann problem. As an example, Roe's Riemann solver [26] is introduced to evaluate the interfacial inviscid fluxes

$$\hat{f}_{i,j} = \frac{1}{2}\left[f^I\left(q^+_{i,j}\right) + f^I\left(q^-_{i,j}\right) - |A|\left(q^+_{i,j} - q^-_{i,j}\right)\right], \tag{2.26}$$

Here $|\mathrm{A}| = R|\Lambda|\mathrm{L}$ with R and L be the right and left eigenvector matrices of the flux Jacobian matrix A, which is defined as

$$A = \frac{\partial f^I}{\partial q} = \begin{pmatrix} 0 & n_x & n_y \\ (c^2 - u^2)n_x - uvn_y & 2un_x + vn_y & un_y \\ -uvn_x - (c^2 - u^2)n_y & vn_x & un_x + 2vn_y \end{pmatrix}. \tag{2.27}$$

This Jacobian matrix has three distinct real eigenvalues. The eigenvalues can be derived analytically. The source term due to the bed slope is dealt with via a revised divergent form method. It has been proved that this method will give physical results even for steady state over complex terrain.

2.3.3. *Examples*

In this section, an example is shown to demonstrate the application of 2D models. This example is the St. Clair River sediment mobility study [19]. Corresponding 3D modeling has also been done to investigate the local flow field and will be introduced in the next section. In the context of this section, only 2D simulation results will be shown.

The St. Clair River is the connecting channel between Lake Michigan-Huron and the downstream Lake St. Clair (Fig. 2.7a, b). Despite the small recovery in year 2009, the head difference between the Michigan-Huron system and Lake Erie has declined by about 0.6 m between 1860 and 2006, with 0.23 m occurring between 1963 and 2006. The level of Lake Erie has remained relatively constant. Among many other hypotheses, the erosion in the St. Clair River and the increased conveyance have been postulated as one of the reasons for the dropping of the water level in Lake Michigan-Huron.

An open-source numerical code, *HydroSed2D*, was applied to the St. Clair River through the reach. *HydroSed2D* is a two-dimensional depth-averaged code that provided detailed

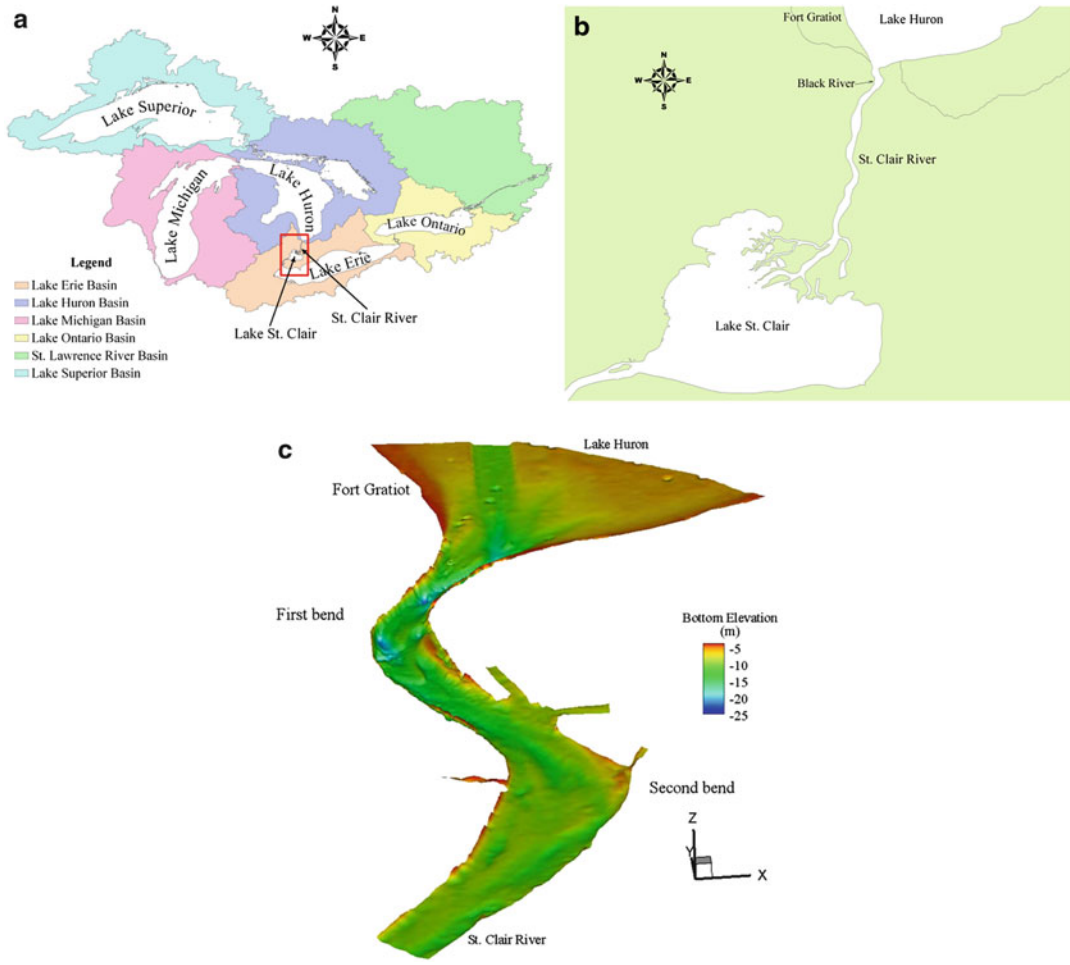

Fig. 2.7. Location and bathymetry of the St. Clair River: (**a**) The Great Lakes region and the St. Clair River. (**b**) The St. Clair River as the connecting channel between Lake Huron and Lake St. Clair. (**c**) Detailed bathymetry of the first two river bends from the multi-beam echo sounding survey.

hydrodynamic predictions (i.e., flow velocity and depth) within the channel [18]. These predictions were then used to calculate sediment transport rates and analyze armoring effects using surface-based gravel bed transport equations based upon the *Acronym* routine [27]. The boundary conditions of the model were based upon detailed field measurements that were conducted on July 21–25, 2008, and combined a multi-beam echo sounder (MBES) bathymetric survey (Fig. 2.7c) and Acoustic Doppler Current Profiler (ADCP) flow velocity surveys [28]. The numerical flow model was also calibrated and validated using these field measurements. The sediment characteristics within the reach (such as size and composition) were obtained through underwater video/image analysis. The bottom shear stresses predicted by *HydroSed2D* and these sediment size distributions were then subsequently used as an input

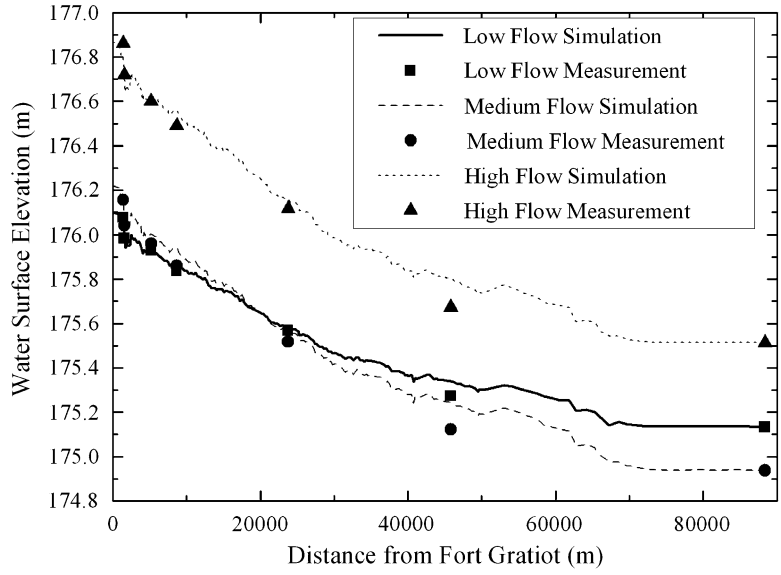

Fig. 2.8. Results for calibrated roughness for the low ($Q = 4{,}645$ m^3/s), medium ($Q = 5{,}282$ m^3/s), and high ($Q = 4{,}645$ m^3/s) flow scenarios.

to *Acronym*. This section demonstrates the integrated modeling approach and presents the results of the analysis, including the distribution of bed shear within the channel, and its implications for the changing water conveyance and lake levels of Lake Michigan-Huron.

All numerical models need extensive calibration before being applied to produce creditable results. In this example, the roughness along the river bottom was chosen as one of the calibration parameters. Due to its importance of hydraulic resistance, many other studies have also used it as the calibration parameter. Some researchers lump the hydraulic resistance into one representative value for the whole domain. However, due to the change of the bed material from upstream to downstream in the St. Clair River, the whole river reach was divided into several subdomains and each of them with a different roughness. The initial estimation of these roughness values are derived from the mean bed material sizes. Different combination of the roughness values for each subdomain constitutes the roughness calibration sets. To cover a wide range of hydraulic conditions, three representative discharges (low, medium, and high) were chosen as the inflow into the river. The simulation results for river stages were compared with the measured results and the best set of roughness were chosen as the calibration result. In Fig. 2.8, the river stages along the St. Clair River with the calibrated roughness are plotted against the measurement. It is clear that the calibrated model can capture the overall hydraulics of the river.

The 2D simulation results were also compared with the ADCP measurement around the first two bends of the river inlet from Lake Huron. In Fig. 2.9, the depth-averaged velocity vectors along several river cross sections are plotted against those from the measurement. The flow discharges during the field measurement and for the simulation are similar. This comparison reveals that the numerical model captured most of the important flow features,

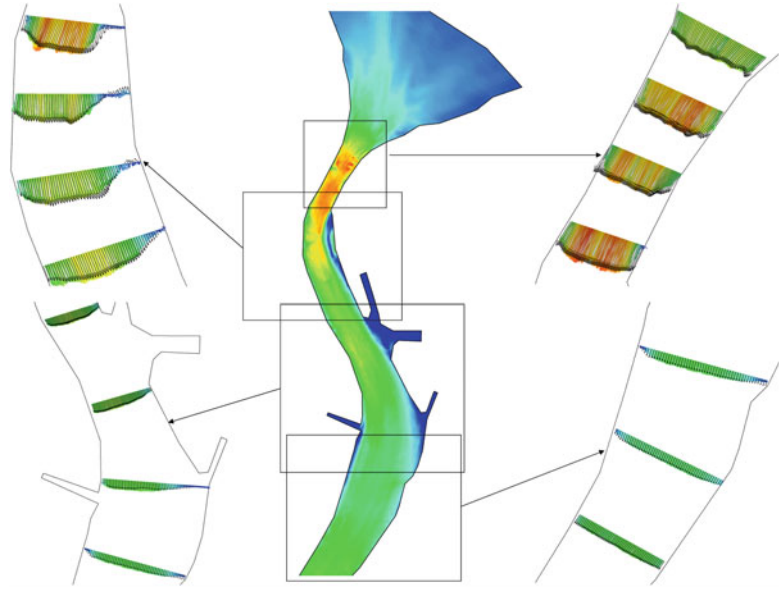

Fig. 2.9. Comparison of depth-averaged velocity vectors between HydroSed2D numerical results and ADCP measurements. The velocity vectors in black are numerical results and those in color are from ADCP measurements.

including the flow constriction and acceleration near the Lake Huron inlet area into the upper river channel and the subsequent large recirculation zone, which extends across approximately a third of the channel width, at the first bend downstream of the constriction. Any morphological change is probably most active within this region, particularly as the downstream flow velocity is accelerated to its maximum within the channel by the influence of both the width constriction and the recirculation zone.

For the purpose of this study, the shear stress exerted on the bed by the flow is the driving force of the sediment motion and is an important parameter to investigate the possible erosion in the river. As a typical flow condition, the case which corresponds to the 50 % exceedance discharge in the flow duration curve is shown in Fig. 2.10. Higher shear stresses are only observed in the St. Clair River channel, with the velocity and shear stresses declining on entry to Lake St. Clair. In the St. Clair River, the highest shear stresses are located in the upper river channel close to Lake Huron outlet. In this area, the bed shear stresses are predicted at about 8–10 Pa. Based upon Shields diagram, this value of shear stress is not capable of moving sediment coarser than 20 mm diameter. However, the shear stresses are high enough to transport finer sediment, with likely deposition in the lee of the first bend of the upper channel, where there are a large outer bank scour and two large lobate bars with shear stresses below 5 Pa through this zone. At this lower value of shear stress, the flow is only able to move sediment finer than 10 mm. The two bars might be historical features from initial water scour. They could still be evolving because of the episodic high shear stresses events such as ship passages and ice jam breakups.

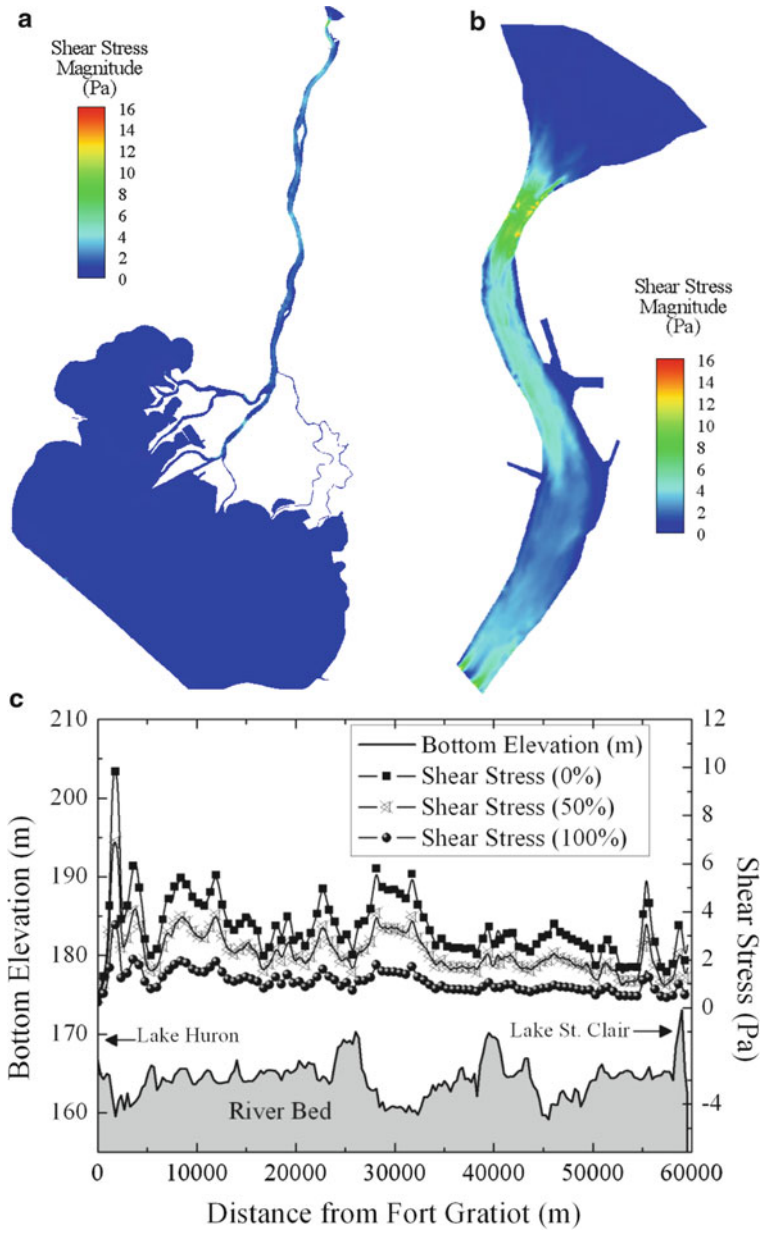

Fig. 2.10. Shear stresses distribution: (**a**) Shear stresses for the whole St. Clair River (50 % flow discharge on the duration curve). (**b**) Shear stresses for the Upper St. Clair River (50 % exceedance flow discharge on the duration curve). (**c**) Shear stresses distributions along the center line of the river (0, 50, and 100 % exceedance flow discharges on the duration curve).

The shear stress distributions corresponding to 0, 50, and 100 % exceedance discharges along the center line of the river (Fig. 2.10c) show that the bed shear stresses decrease downstream from peaks near the Lake Huron outlet, at the location of constriction. However, it is notable that, in general, the bed shear stresses along most of the length of the river are globally low, ranging in mean values from 1 to 3 Pa. It is concluded from the 2D numerical simulation results that the St. Clair River itself can not cause enough erosion to dramatically change the conveyance of the river. Other factors, such as navigation and dredging activities, may play a more important role.

2.4. Three-Dimensional CFD Modeling of Open-Channel Flows

2.4.1. Governing Equations of 3D Navier–Stokes Equations

To do fully three-dimensional modeling of open-channel flows, there are several questions need to be answered regarding to the important physical processes involved.

The first question is the turbulence. Since the Reynolds number, which is a dimensionless number measuring the ratio between the inertial and viscous force, is usually very high due to the large spatial scales in open channels, the flow is dominated by inertial force and turbulent. To directly resolve all the scales in the turbulent flow without modeling is a tremendous challenge and is only possible for relatively moderate Reynolds numbers and simple geometries. Instead, the governing equations are usually averaged/filtered over time and/or space. Most numerical methods used to solve the averaged/filtered equations can only resolve the turbulence up to the scales comparable to the mesh size. Turbulence models are needed to represent the scales which are not resolved. Interested readers could refer to the abundant literatures on this topic, for example, [29–31], among many others.

The second question is the modeling of the free surface in the open channel. For open-channel flows, either the traditional river flows, coastal flows, or the flows through hydraulic structures, part of the flow boundary directly contacts with the atmosphere and is free to move. Under some circumstances, the whole domain occupied by the water and air could be confined in a limited space, for example, partially filled sewage pipe flows where air, though compressible, could retard the free motion of the water surface. In any case, the interface between water and air evolves with time and is part of the solution. The resolution of the free surface introduces extra computational complexity into the problem [32], although mature numerical schemes are available to track or capture the free surface, such as volume of fluid (VOF, [33]) and level set method (LSM, [34]). In practice, unless absolutely necessary, free water surface is usually replaced by a rigid lid where the surface is replaced by a shear-free boundary. This is a good approximation when the free surface does not change dramatically. For rapidly changing water surface (e.g., waves and hydraulic jumps), the rigid lid approximation will introduce errors and should not be used.

Based on the specific problem to be solved, the best strategy is to identify the most important fluid dynamics processes and choose the modeling approach accordingly. The aim is to reduce the unnecessary computational demand while capturing the physical phenomenon. In the following part of this section, the governing equations with the most commonly used turbulence model will be introduced. And then the numerical methods and

codes available will be briefly described. At the end of this section, examples of 3D CFD modeling of the open-channel flows will be shown.

To be general, we assume the resolution of the free surface is important and use the VOF method as an example. In the VOF method, a scalar transport equation is solved as an indicator for the water and air where a value of 1 represents water and 0 represents air. If the free surface is not as important, the VOF scheme could be easily turned off by not solving the scalar transport equation and fill the whole domain by a value of 1. The interface between water and air could be replaced by a rigid lid. The governing equations for the fluid are the Reynolds-averaged Navier–Stokes equations:

$$\frac{\partial \rho}{\partial t} + \nabla \cdot (\rho u) = 0, \tag{2.28}$$

$$\frac{\partial \rho u}{\partial t} + \nabla \cdot (\rho u u) - \nabla \cdot [(\mu + \mu_{\mathrm{t}})\overline{\overline{\sigma}}] = -\nabla p + \rho g \tag{2.29}$$

where u is the fluid velocity vector field, p is the pressure field, μ is the molecular viscosity, μ_{t} is the turbulent eddy viscosity, $\overline{\overline{\sigma}}$ is the strain rate tensor, and g is the gravity force vector. The density ρ in the domain is given by

$$\rho = \alpha \rho_{\mathrm{w}} + (1 - \alpha)\rho_{\mathrm{a}}, \tag{2.30}$$

where α is the volume fraction of water and ρ_{w} and ρ_{a} are densities of water and air, respectively.

The volume fraction scalar, α, is governed by the transport equation which has the form

$$\frac{\partial \alpha}{\partial t} + \nabla \cdot (\alpha u) = \mu \nabla^2 \alpha. \tag{2.31}$$

To solve the turbulent eddy viscosity μ_{t}, turbulence models need to be used. As an example, equations for fluid model are closed by the conventional k-ε turbulence model [35], which is most popular in engineering practice,

$$\mu_{\mathrm{t}} = C_{\mu} \rho \frac{k^2}{\varepsilon}, \tag{2.32}$$

$$\frac{\partial k}{\partial t} + \nabla \cdot [uk] = \frac{1}{\rho} \nabla \left(\frac{\mu_{\mathrm{t}}}{\sigma_k} \nabla k \right) + 2 \frac{\mu_{\mathrm{t}}}{\rho} |\nabla u|^2 - \varepsilon, \tag{2.33}$$

$$\frac{\partial \varepsilon}{\partial t} + \nabla \cdot [u\varepsilon] = \frac{1}{\rho} \nabla \left(\frac{\mu_{\mathrm{t}}}{\sigma_k} \nabla \varepsilon \right) + 2 \frac{C_1 \mu_{\mathrm{t}}}{\rho} |\nabla u|^2 \frac{\varepsilon}{k} - C_2 \frac{\varepsilon^2}{k}, \tag{2.34}$$

where k is turbulence kinetic energy and ε is turbulence energy dissipation rate and σ_k and σ_ε are the Schmidt numbers. The constants appear in (2.20)–(2.22) take the values of $C_\mu = 0.09$, $C_1 = 1.44$, and $C_2 = 1.92$ [35]. The Schmidt numbers have the values of $\sigma_k = 1.0$ and $\sigma_\varepsilon = 1.0$. More turbulence models can be found in the literature.

2.4.2. Numerical Solutions and Available Codes

The partial differential equations (PDEs) of the 3D CFD models can be solved using any numerical schemes (e.g., finite-difference, finite element, and finite volume methods) introduced in the previous sections. Whatever the schemes chosen, the PDEs are discretized and the physical variables (velocity, pressure, etc.) are solved at finite number of grid points. As mentioned in the introduction, in general, the process includes preprocessing, simulation, and post-processing. A very important step in the preprocessing stage is to prepare a good quality mesh which can determine the overall quality of simulation results and sometimes even the success or failure of the simulation.

There are a number of commercially available programs such as Fluent, Flow3D, Phoenics, and CD-adapco which are used widely in practice because of their ease of use and good support. In recent years, with the growth of the open-source movement (from operating systems to applications), several CFD codes are released under various open-source license agreements. Instead of compiled binary executables as is the case with most of the commercial codes, the whole source code is available. This is very appealing to people who wish to have the freedom to modify the code according to his or her particular application. The drawback of open-source CFD codes is that the learning curve is steep and it needs more background and experience in computer programming.

One of the popular open-source CFD code is OpenFOAM [36], which has been used extensively by the author for various applications. OpenFOAM is primarily designed for problems in continuum mechanics. It uses the tensorial approach and object-oriented techniques [37]. OpenFOAM provides a fundamental platform to write new solvers for different problems as long as the problem can be written in tensorial partial differential equation form. It comes with a large number of turbulence models for both incompressible and compressible fluids. The core of this code is the finite volume discretization of the governing equations. Differential operators in a partial differential equation, such as temporal derivative, divergence, Laplacian operator, and curl, can be discretized in the code. A numerical solver which solves the partial differential equations can be written at high programming level with great efficiency. Researchers and engineers can be liberated from the burden of tedious coding and focus on the physical problem. In the next section, an example of 3D CFD simulation using OpenFOAM will be introduced.

2.4.3. Examples

Three-dimensional computational models have been used in many applications involving almost all aspects of traditional and emerging open-channel hydraulics problems. Some of the examples include secondary flows in meandering channels, turbulent coherent structures over complex bed forms and rough elements such as gravels, and free surface flow through/around

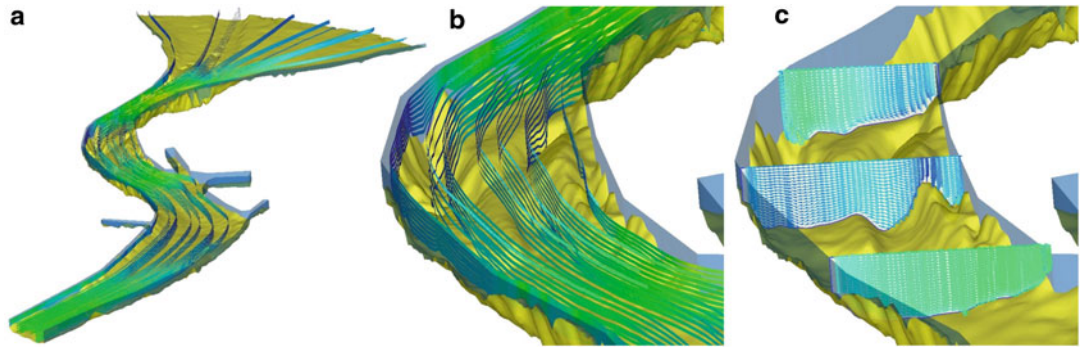

Fig. 2.11. Streamlines and velocity vector plots around the first two bends of the St. Clair River: (**a**) Streamlines around the first two bends from Lake Huron to the St. Clair River. (**b**) Streamlines over the bedforms in the first bend. (**c**) Secondary flow in the first bend over the bedforms.

hydraulic structures such as spillways and fish passages. If the channel is built with a mobile bed, sediment transport and channel evolution can also be modeled together with the fluid flows. In this section, an example will be shown to demonstrate the application of three-dimensional numerical modeling of open-channel flows. This example is the 3D sediment mobility analysis in the St. Clair River, whose 2D analysis has been introduced in the previous section.

As we have seen in the previous section of 2D depth-averaged models, St. Clair River was modeled using finite volume shallow-water equations. To further understand the hydraulics of the river, especially at the river inlet from Lake Huron where it could be most active morphologically, 3D CFD simulation was performed. The 3D simulation results could also be used to cross-check the 2D model.

Due to the limitation of computational resource, only the Lake Huron inlet area and the first two bends are modeled in the 3D simulations. The bathymetry is from the multi-beam scan and the 3D view of the 2008 bathymetry is show in Fig. 2.7. The domain is about 8 km long and it has a mesh of about 1.5 million cells. The turbulence is modeled by the k-ε model. Although surface waves in the lake inlet area present, the river surface elevations of the majority of the domain only changes slightly. Thus, a rigid lid is placed on the top of domain. It takes more than 24 h for the model to reach steady state in an eight nodes computer cluster.

The flow pattern from the 3D model is shown in Fig. 2.11. The stream traces in Fig. 2.11a, b help visualize the flow field. In the first bend, the velocity vectors in several cross sections are shown in Fig. 2.11c. The secondary flow feature is evident. This may cause the further scour of the deep hole on the outer bend and deposit sediment on the two sandbars in the inner bend. The flow field from the numerical model with 3D ADCP measurement can be used to give a clear picture of what is happening around the bend.

The comparison of the bed shear stress between the 2D and 3D models is shown in Fig. 2.12. Although exact match of the shear stresses is not possible, the basic patterns of the shear distribution from both models agree well. For both models, the maximum shear stress is located at the Lake Huron inlet area, and in the second bend, low shear stress is

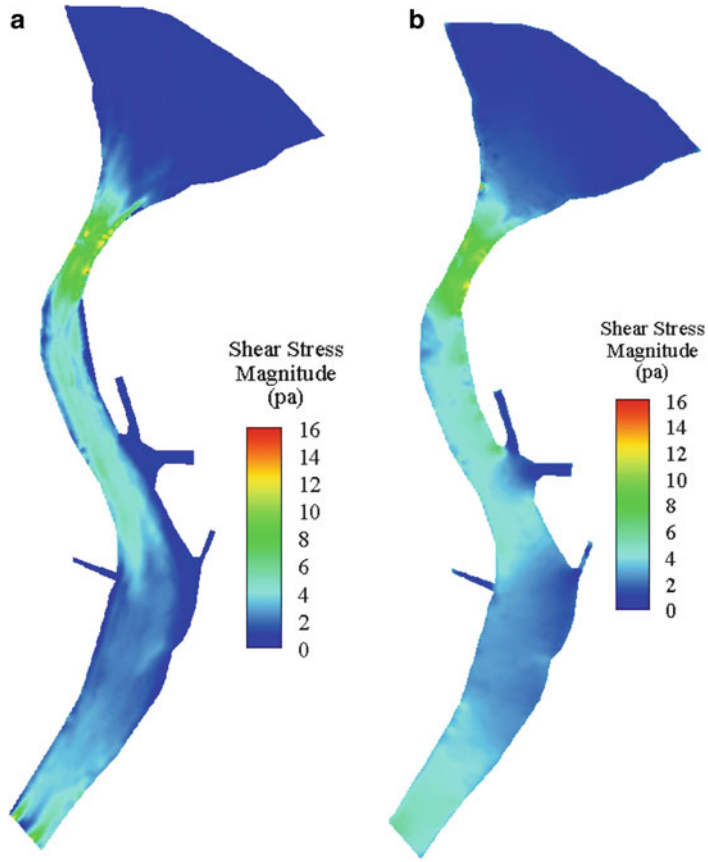

Fig. 2.12. Comparison on the bed shear stress between 2D modeling (HydroSed2D) and 3D modeling (OpenFOAM) around the first two bends of the St. Clair River: (**a**) Results from HydroSed2D. (**b**) Results from OpenFOAM.

observed. The magnitude of the shear stress also agrees well indicating the roughness coefficient selected and the velocity magnitudes the model computed are in the right range. With these, it is reasonable to conclude that the HydroSed2D model gives reasonable results.

3. MODERN AND FUTURE CHALLENGES

As has been the case with most engineering disciplines, the major advances in open-channel hydraulics in the past five decades have been in areas digital computing and software development. To assert there were no advances in theory and understanding of the governing processes would be wrong; but those advancements have not had the impact that the advances in computing have had. The advances in computing power and software are now permitting water resource engineers to examine complex, multidisciplinary problems that could previously only be considered qualitatively. Among the problems involving open-channel

hydraulics problems are the following, and it is pertinent to observe that they require multidisciplinary approaches which synthesize the skills and knowledge of professionals in diverse fields to develop solutions. Or to paraphrase the old adage, the solution is greater than the sum of its components.

3.1. Revisiting Past Projects

Throughout the 1950s and 1960s in the United States, many natural channels were straightened and lined to increase their hydraulic efficiency in conveying flood flows. While these improvements maximized conveyance, they often resulted in channels that are by current standards less than ideal for a number of reasons and among them are the following. Many improved channels are aesthetically unappealing; that is, they are usually prismatic, straight, functionally lined with concrete or a similar artificial material, and protected with chain-link fence. The channel pictured in Fig. 2.4 is an example of a functional but is not aesthetically pleasing nor was it intended to be. In 1954, the US Army Corps of Engineers undertook the San Antonio Channel Improvements Project, and during the early stages of this project in the 1950s and 1960s, the San Antonio River below the downtown was straitened to efficiently convey flood flows through densely populated areas. In the twenty-first century portions of that reach of the San Antonio River are being restored to achieve better aesthetics, restore riparian areas, and provide for recreation while maintaining hydraulic conveyance.

In discussing preserving natural channels while mitigating flood flows, Indian Bend Wash in Scottsdale, AZ, must be mentioned. Indian Bend Wash is an ephemeral channel that bisects the City of Scottsdale. Before 1960, Scottsdale was a rural agricultural community that could not afford to bridge a channel that rarely conveyed flow. However, during the 1960s, there were a series of severe floods and Federal tax dollars were allocated for US Army Corps of Engineers to remedy the problem. The proposed remedy was to build a prismatic concrete canal instead of a system of parks and golf courses the community wanted. Grass was an untried lining for channels conveying episodic flows and high maintenance costs were anticipated. The City, in a controversial and bold move, voted for flood mitigation by the aesthetically attractive system of parks and golf courses which today is known as Scottsdale Greenbelt. This project, built against the Corps of Engineers judgment, has proved to be a success from the viewpoints of flood mitigation, aesthetics, and recreation.

Restoring or maintaining channels to mitigate flood flows and achieve other design objectives is a challenging problem that requires a multidisciplinary approach. In restoring a channel, a stable section must be designed and constructed that behaves under many flow regimes as a natural channel that took decades to form. It is pertinent to observe that the approaches to this challenge can, generally, be divided into two groups: qualitative and quantitative. The quantitative approaches derive from the theory of sediment transport and river mechanics. This is the preferred approach of professionals who have backgrounds in deterministic Newtonian mechanics. The qualitative approach is generally favored by people whose background is not mechanics and views watershed management holistically; see, for

example, [38]. The proponents of the two approaches both dismiss the merits and validity of other approach while asserting theirs is valid. Restoring a disturbed system to a "natural" condition that is in equilibrium is a challenge for which there is not yet a sufficient or adequate understanding of the processes involved.

Managing a natural floodway in an urban environment is also a multidisciplinary challenge. That is, melding the needs to maintain conveyance and riparian habitat while enhancing recreation and preventing the spread of nonnative invasive species is a complex technical and social issue. A technical issue that remains a challenge is estimating the Manning resistance coefficient for naturally vegetated areas with diverse ground cover and vegetation. Although progress has been made in this area, see, for example, [39, 40], more work is needed. A second and equally important issue is balancing the hydraulic conveyance needed with maintaining health and diverse riparian areas; see, for example, [41]. Finally, other uses of the channel and its floodplain must often be considered such as recreation, that is, hiking and biking trails, parks, and playing fields.

3.2. Effects of Climate Variability

Without entering into a discussion of whether there will be significant climate change in the near future or not, the water resource engineers treat the variability of climate and weather in designing and maintaining open-channel systems. One of the most important sources of year-to-year climate variation throughout the world is the El Niño/La Niña phenomena of the tropical Pacific Ocean. Under normal conditions, the tropical trade winds blow from the east to west resulting in the concentration of warm water in the western Pacific Ocean. In the eastern Pacific Ocean, the effect of the trade winds is to upwell cold, deep nutrient waters along the Equator from the coast of Ecuador to the Central Pacific. During an El Niño episode, the trade winds weaken and the upwelling of the cool waters in the Eastern Pacific is reduced. In turn, this allows the warm water in the Western Pacific to drift eastward towards South America. As the central and eastern Pacific warms, atmospheric pressure gradients along the Equator weaken and the trade winds are further diminished. These changes are the defining factors of an El Nino episode and were first noted by Gilbert Walker in the early decades of the twentieth century who termed this the "Southern Oscillation." From the viewpoint of water resources engineering in the United States, the importance of this cycle is that during El Niño periods, the Southwest tends to be wet and the Northwest dry and vice versa for La Niña periods. The implications of the El Niño/La Niña phenomena on water supply are known and have been studied; see, for example, [42]. However, the implications of these phenomena on flood mitigation projects, in general, and open channels, in particular, have not been studied in any detail.

From the viewpoints of designing and maintaining open-channel systems, whether the climate is changing on an engineering timescale is less important than whether climate and weather variability have been properly taken into account. This is again an area where the water resources engineer can form productive partnerships with professionals in the geosciences, statistics, and atmospheric sciences to reduce both cost and risk.

3.3. Challenges of Natural Open Channels in the Arid Environment

Flow in open channels in the arid environment present a unique challenge since the flows are often episodic and flood hazard is often less related to magnitude than to quickness and ferocity. In addition, non-Newtonian flows of mud and debris are common in some areas and unconfined flows are common. The dominant landform in semiarid and arid environments is the alluvial fan. For example, in the southwestern United States, alluvial fans and bajadas occupy approximately 31.3 % of the area [43]. From the viewpoint of water resources engineering, an appropriate definition is that of the US Federal Emergency Management Agency (FEMA) [44] or

> Alluvial fans are geomorphic features characterized by cone-or fan shaped deposits of boulders, gravel, sand, and fine sediments that have been eroded from mountain watersheds, and then deposited on the adjacent valley floor... Flooding that occurs on active alluvial fans is characterized by fast-moving debris and sediment laden shallow flows. The paths followed by these flows are prone to lateral migration and sudden relocation to other portions of the fan. In addition, these fast moving flows present hazards associated with erosion, debris flow, and sediment transport.

The FEMA definition itemizes the hydraulic processes expected to occur on a generic, regulatory alluvial fan from an engineering viewpoint; and this definition makes clear that hazards on alluvial fans are due to a wide range of hydraulic processes that involve sediment movement and transport; and many of these processes are not yet well understood.

While hydraulic processes on alluvial fans have interested those in the geosciences for many years, the interest of the engineering community began when development on alluvial fans rose to a level where the hazards of flooding on these landforms could not be ignored. The seminal paper treating open channels conveying floods on alluvial fans was [45] which proposed a probabilistic approach to flood hazard identification and mitigation on alluvial fans. Since 1979, a vigorous debate, often acrimonious, over modeling open-channel flow on alluvial fans has taken place. Although sophisticated two-dimensional models, see [46] for example, a consensus, either technical or regulatory, has been reached. Again this is a problem involving both the engineering and geoscience communities and should be addressed jointly.

3.4. Discovering and Implementing New Synergies

The foregoing sections have suggested critical topics involving open channels where the knowledge available is not sufficient to address critical problems that require solutions. In almost all cases these problems are at the interface between engineering and one or more of the sciences: geology, geomorphology, ecology, or hydrometeorology to name just a few. The advancements in modeling over the past several decades have reached the point that synergetic considerations covering multiple disciplines are possible and necessary. In this aspect, model integration becomes important and inter-model communication should be standardize to ensure smooth flow of data and information. Future generations of computational hydraulics modeling tools should also incorporate the emerging technologies such as cloud computing and big data processing to improve efficiency and accuracy. The boundary between model and data will probably be blurred furthermore which requires the adaptation of our modeling philosophy.

REFERENCES

1. Rouse H, Ince S (1957) History of hydraulics. Dover Publications, New York
2. Reisner M (1986) Cadillac Desert. Viking Penguin, Inc., New York
3. Kahrl WL (1982) Water and power: the conflict over Los Angeles water supply in the Owens Valley. University of California Press, Berkeley, CA
4. USACE (2010) HEC-RAS river analysis system, hydraulic reference manual. US Army Corps of Engineers Hydrologic Engineering Center, Davis, CA
5. FHA (2000) Chapter 8: stilling basins. Hydraulic design of energy dissipators for culverts and channels, hydraulic engineering circular no. 14, 3rd edn 2. Federal Highway Administration, Washington DC
6. Wei CY, Lindell JE (1999) Chapter 18: hydraulic design of stilling basins and energy dissipators. In: Mays LW (ed) Hydraulic design handbook. McGraw-Hill, New York, NY
7. Levi E (1995) The science of water: the foundation of modern hydraulics. American Society of Civil Engineers, New York, NY
8. Herschel C (1897) 115 Experiments on the carrying capacity of large, Riveted Metal Conduits (Google books). Robert Drummond, Electrotyper and Printer, New York
9. Flamant A (1900) Hydraulique (Google books), 2nd edn. Beranger, Paris
10. Fischenich C (2000) Robert manning (a historical perspective), ERDC TN-EMRRP-SR-10. U.S. Army Engineer Research and Development Center, Environmental Laboratory, Vicksburg, MS
11. King HW (1918) Handbook of hydraulics for the solution of hydraulic problems. McGraw-Hill, New York
12. Sturm TW (2010) Open channel hydraulics, 2nd edn. McGraw Hill Higher Education, Burr Ridge, IL
13. Mays LW (2005) Water resources engineering. Wiley, Berlin
14. U.S. Army Corps of Engineers (2003) Subquehanna River flood warning and response system. Project report PR-56. U.S. Army Corps of Engineers, Hydrologic Engineering Center, Davis, CA
15. Tate EC, Maidment DR, Olivera F, Anderson DJ (2002) Creating a terrain model for floodplain mapping. J Hydrol Eng 7(2):100–108
16. Bermúdez A, Rodríguez C, Vilar MA (1991) Solving shallow water equations by a mixed implicit finite element method. IMA J Numer Anal 11(1):79–97
17. Bradford SF, Sanders BF (2002) Finite-volume model for shallow-water flooding of arbitray topography. J Hydraul Eng 128(3):289–298
18. Weiming W (2004) Depth-averaged 2-D numerical modeling of unsteady flow and nonuniform sediment transport in open channels. J Hydraul Eng 130(10):1013–1024
19. Liu X, García MH (2008) Coupled two-dimensional model for scour based on shallow water equations with unstructured mesh. Coast Eng 55(10):800–810
20. Liu X, Parker G, Czuba J, Oberg K, Mier JM, Best JL, Parsons DR, Ashmore P, Garcia MH (2011) Sediment Mobility and Bed Armoring in the St. Clair River: insights from hydrodynamic modeling. Earth Surface Processes and Landform 37(9):957–970
21. Fujihara M, Borthwick AGL (2000) Godunov-type solution of curvilinear shallow-water equations. J Hydraul Eng 126(11):827–836
22. Borthwick AGL, León SC, Józsa J (2001) Adaptive quadtree model of shallow-water hydrodynamics. J Hydraul Res 39(4):413–424
23. Galland JC, Goutal N, Hervouet JM (1991) TELEMAC—a new numerical model for solving shall-water equations. Adv Water Resour 14(3):138–148
24. TUFLOW (2008) TUFlOW user manual, GIS based 2D/1D hydrodynamic modelling, TUFLOW

25. Godunov SK (1959) A difference scheme for numerical solution of discontinuous solution of hydrodynamic equations. Math Sbornik 47:271–306, translated US Joint Publ. Res. Service, JPRS 7226, 1969
26. Hirsch C (1990) Numerical computation of internal and external flows. Computational methods for inviscid and viscous flows, vol 2, Wiley series in numerical method in engineering. Wiley, Berlin
27. Roe PL (1981) Approximate Riemann solvers, parameter vectors, and difference schemes. J Comput Phys 43:357–372
28. Parker G (1990) Surface-based bedload transport relation for gravel rivers. J Hydraul Res 28(4):417–436
29. Czuba JA, Oberg KA, Best J, Parsons DR (2009) The effect of channel shape, bed morphology, and shipwrecks on flow velocities in the Upper St. Clair River. Proceedings of 33rd IAHR congress, Vancouver, BC, Canada
30. Tennekes H, Lumley JL (1972) A first course in turbulence. MIT Press, Cambridge, MA
31. Sagaut P (2001) Large eddy simulation for incompressible flows: an introduction. Springer, Berlin
32. Wilcox DC (2006) Turbulence modeling for CFD, 3rd edn. DCW Industries, La Canada, CA
33. Liu X, García MH (2008) A 3D numerical model with free water surface and mesh deformation for local sediment scour. J Waterw Port Coast Ocean Eng 134(4):203–217
34. Hirt CW, Nichols BD (1981) Volume of fluid (vof) method for dynamics of free boundaries. J Comput Phys 39(1):201–225
35. Sethian JA (1996) Level set methods: evolving interfaces in geometry, fluid mechanics, computer vision, and material science, Cambridge monographs on applied and computational mathematics. Cambridge University Press, Cambridge
36. Rodi W (1980) Turbulence models and their applications in hydraulics. IAHR monograph series. Rotterdam, Brookfield, A.A. Balkema
37. OpenCFD (2010) Openfoam: the open source computational fluid dynamics (CFD) toolbox. http://www.OpenFoam.org
38. Weller HG, Tabor G, Jasak H, Fureby C (1998) A tensorial approach to computational continuum mechanics using object-oriented techniques. Comput Phys 12(6):620–631
39. Rosgen DL, Silvey HL (1996) Applied river morphology. Wildland Hydrology Books, Fort Collins, CO
40. Flippin-Dudley SJ, Abt SR, Bonham CD, Watson CC, Fischenich JC (1997) A point quadrant method of vegetation measurement for estimating flow resistance. Technical Report EL-97–XX. U.S. Army Waterways Experiment Station, Vicksburg, MS
41. Kouwen N, Fathi-Moghadam M (2000) Friction factors for coniferous trees along rivers. J Hydraul Eng ASCE 126(10):732–740
42. Murray KE, Bush JK, Haschenburger JK, French RH (2008) Technical and field guide: management practices for natural waterways. Center for Water Research, University of Texas at San Antonio, San Antonio, TX
43. Cayan DR, Peterson DH (1989) The influence of North Pacific circulation on streamflow in the West. Aspects of climate variability in the Pacific and Western Americas. Geophys Monogr 55:375–398
44. Anstey RL (1965) Physical characteristics of alluvial fans, Technical Report ES-20. US Army Natick Laboratories, Natick, MA
45. Federal Register (1989) 54(156)
46. Dawdy DR (1979) Flood frequency estimates on alluvial fans. J Hydraul Div Proc Am Soc Civil Eng 105(HY11):1047

http://www.springer.com/978-1-62703-594-1

Modern Water Resources Engineering
Wang, L.K.; Yang, C.T. (Eds.)
2014, XX, 866 p. 248 illus., 155 illus. in color.,
Hardcover
ISBN: 978-1-62703-594-1
A product of Humana Press